

DOI: 10.1002/adem.201500073

# Effect of Strain Rate on Tensile Ductility and Fracture Behavior of Bulk Nanotwinned Copper\*\*

By Zesheng You and Lei Lu\*

*A bulk columnar-grained copper with preferentially oriented nanoscale growth twins is prepared by means of direct-current electrodeposition. Tensile tests at different strain rates reveal a significant influence of strain rate on the tensile ductility and fracture behavior. The ductility, especially the post-necking elongation, reduces dramatically at low strain rates, which is associated with evident intergranular fracture. The results suggest that the grain size as well as the grain boundary microstructural evolution exert a strong influence on the intrinsic fracture mode in the nanotwinned structure.*

Hierarchical microstructure with nanoscale twin boundaries (TBs) incorporated into polycrystalline metals has attracted world-wide attention over the past decade, as the nanotwinned structure simultaneously exhibits several superior mechanical properties, including ultra-high strength, good ductility, and enhanced work hardening.<sup>[1–6]</sup> It has been accepted that the coherent TBs at the nanoscale play an essential role in generating the outstanding properties not only by obstructing motion of dislocations but also by providing ample space for dislocation storage.<sup>[1,7]</sup> Intrinsic microstructure characteristics, including twin length (i.e., grain size) and twin thickness, affect the mechanical properties as well as the plastic deformation mechanisms.<sup>[8–10]</sup> Recently, via a columnar-grained Cu with nanoscale growth TBs preferentially oriented parallel to the deposition plane, it is further instructive to detect the fact that TB orientation with respect to the loading direction could substantially affect the dominating dislocation mechanism for

both monotonic and cyclic deformation.<sup>[11–13]</sup> For instance, if TBs are mostly aligned with tensile direction, the plastic deformation is mainly accomplished by threading dislocations nucleating from grain boundaries (GBs) and bowing out under the constraint of neighboring TBs.<sup>[12,14]</sup>

Strain rate effect on plastic flow behavior is generally studied in order to reveal the intrinsic deformation mechanism of metallic materials.<sup>[15–17]</sup> Through systematically investigating the strain rate sensitivity of nanotwinned Cu (nt-Cu) with randomly oriented nanoscale twins, Lu *et al.* demonstrated a substantially elevated strain rate sensitivity contributed by strong dislocation–TB interactions as the twin thickness was reduced down to tens of nanometer.<sup>[18–20]</sup> For the nt-Cu with highly oriented nanoscale twins, Ye *et al.* demonstrated a TB orientation dependence of strain rate sensitivity, a reflection of the intrinsic plastic anisotropy.<sup>[21]</sup> On the other hand, tensile tests at different strain rates only revealed a slightly enhanced ductility with increasing strain rate.<sup>[18,22]</sup>

The previous studies of strain rate effect on the mechanical response of nanotwinned structure have mainly dealt with samples with grains in the nanometer and submicron meter scale ( $\leq 500$  nm). However, it has also been demonstrated that GBs can interact with impinging dislocations, leading to strong dependences of strain hardening and ductility on grain size.<sup>[11,23]</sup> Therefore, the strain rate effect might become starkly different in nanotwinned structure with large grains in the micrometer scale.

In this study, we prepared a bulk nt-Cu with micrometer-sized grains by a direct-current electrodeposition technique and investigated the influence of strain rate on the tensile behavior. The work is aimed at developing a much deeper understanding of the GB deformation behavior and its relationship with macroscopic properties of this special hierarchical nanostructure.

[\*] Prof. L. Lu, Dr. Z. You

Shenyang National Laboratory for Materials Science, Institute of Metal Research, Chinese Academy of Sciences, 72 Wenhua Road, Shenyang 110016, People's Republic of China  
E-mail: llu@imr.ac.cn

Dr. Z. You

Herbert Gleiter Institute of Nanoscience, Nanjing University of Science and Technology, 200 Xiaolingwei Street, Nanjing 210094, People's Republic of China

[\*\*] The authors acknowledge financial support from the National Basic Research Program of China (973 Program, 2012CB932202), the National Science Foundation of China (Grant Nos. 51420105001, 51371171, 51471172, and 51401211). L.L. thanks the financial support of the "Hundreds of Talents Project" by the Chinese Academy of Sciences.

The typical microstructure of the as-deposited nt-Cu is shown in Figure 1. It can be seen from the plane-view scanning electron microscope (SEM) observations (Figure 1a) that the polycrystalline grains are homogeneous and equiaxed, with a diameter ranging from 3 to 10  $\mu\text{m}$ . The average grain size is  $\approx 6 \mu\text{m}$ , which is about one to two orders of magnitude larger than that of the samples prepared by pulse electrodeposition and by magnetron sputtering.<sup>[22,24–26]</sup> Cross-sectional observations in Figure 1b show that the grains are in fact columnar in shape with longitudinal length between 50 and 200  $\mu\text{m}$ , much larger than the transverse diameter. High-density nanoscale growth twins, mostly oriented parallel to the deposition plane, are clearly seen inside the grains. Statistics on transmission electron microscope images indicate an average twin thickness of  $\approx 70 \text{ nm}$ .

Figure 2 shows the tensile engineering stress–strain curves of the nt-Cu at different strain rates. Evidently, changing the strain rate exerts a strong influence on the mechanical response of the nt-Cu. The yield stress ( $\sigma_y$ ) increases from 240 to 300 MPa as the strain rate elevates from  $10^{-5}$  to  $10^{-2} \text{ s}^{-1}$ , while the ultimate tensile stress ( $\sigma_{\text{uts}}$ ) increases from 290 to

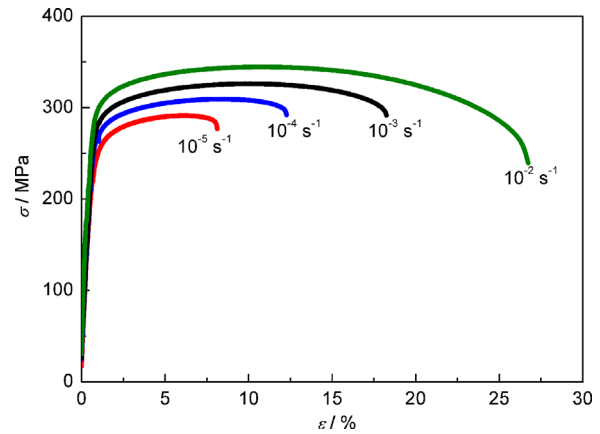


Fig. 2. Tensile engineering stress–strain curves of columnar-grained nt-Cu tested at different strain rates, ranging from  $10^{-5}$  to  $10^{-2} \text{ s}^{-1}$ .

350 MPa. The strain hardening capacity, usually defined as  $H_c = \sigma_{\text{uts}} / \sigma_y$ , remains at  $\approx 1.20$  for all the strain rates, suggesting a relatively limited influence of strain rate on the strain hardening. From the tensile results at different strain rates, the strain rate sensitivity  $m$  of the flow stress is estimated to be  $\approx 0.02$ , by using the equation  $m = \partial \ln \sigma / \partial \ln \dot{\epsilon}$ . This result is in good agreement with the findings by Lu *et al.* on a electrodeposited medium twin density sample ( $m = \approx 0.026$ ) and by Hodge *et al.* on a similar columnar-grained nt-Cu ( $m = \approx 0.021$ ) prepared by magnetron sputtering.<sup>[18,22]</sup>

It is more noteworthy in Figure 2 that increasing strain rate can substantially enhance the tensile ductility of the nt-Cu as well. At a strain rate of  $10^{-5} \text{ s}^{-1}$ , the elongation-to-failure ( $\delta_f$ ) is only 9%; however,  $\delta_f$  is as high as 28% if the sample is tensioned at  $10^{-2} \text{ s}^{-1}$ . The uniform elongation ( $\delta_u$ ) also increases with strain rate, but its increment is much smaller than that of  $\delta_f$ , i.e., only from  $\approx 6$  to  $\approx 11\%$ . The variations of  $\delta_u$  and  $\delta_f$  as a function of the imposed strain rate are summarized in Figure 3. Clearly, the influence of strain rate on the tensile ductility appears to lie majorly in the post-necking elongation,

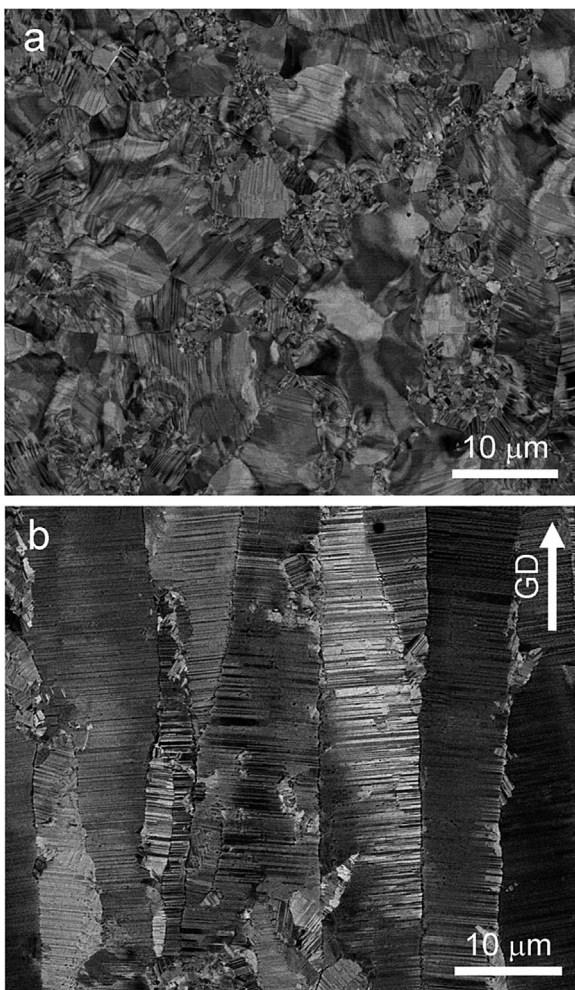


Fig. 1. SEM micrographs of the as-deposited nt-Cu: (a) plane-view observation; (b) cross-section observation. The white arrow GD in (b) indicates the growth direction.

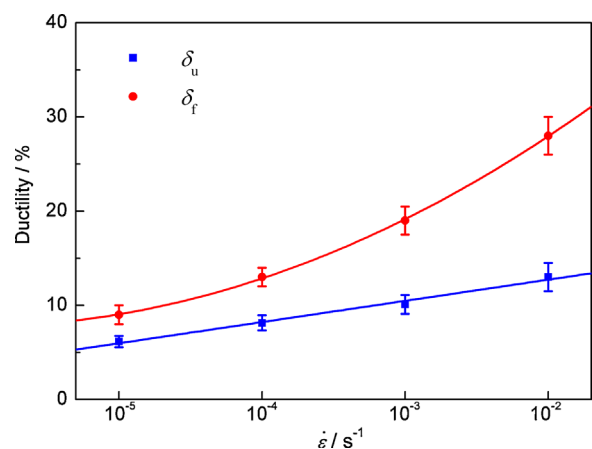


Fig. 3. Variations of uniform elongation  $\delta_u$  and elongation-to-failure  $\delta_f$  of columnar-grained nt-Cu as a function of strain rate  $\dot{\epsilon}$ .

$\delta_{pn} = \delta_f - \delta_u$ .  $\delta_{pn}$  is only  $\approx 3\%$  when the sample is tested at  $10^{-5} \text{ s}^{-1}$ , indicating that the sample fractures shortly after the commencement of localized necking. Instead, the necking and eventual fracture are substantially suppressed by tensioning the sample at higher strain rates, which results in a  $\delta_{pn}$  of  $\approx 17\%$  at  $10^{-2} \text{ s}^{-1}$ , over five times that at low strain rates. The dependence of tensile ductility upon strain rate in nt-Cu with micrometer-sized grains is rather different from the case with submicron- and nano-meter grains.<sup>[18,22]</sup>

The plane and side faces of fractured specimens tested at different strain rates are shown in Figure 4, which also clearly demonstrate the substantial influence of strain rate on the deformation capability. As shown in Figure 4a, almost no necking can be observed on the sample plane at the lowest strain rate ( $10^{-5} \text{ s}^{-1}$ ). The sample breaks along a sharp shear plane with an angle of  $55^\circ$  with respect to the tensile direction. With increase in strain rate, the necking extent significantly

increases (Figure 3b–d). The true plastic strain  $\epsilon_w$  in the width direction, defined as  $\ln(w_0/w)$ , where  $w_0$  and  $w$  are the original and final width at the fracture, respectively, increases from 12 to 57% with strain rate increasing from  $10^{-5}$  to  $10^{-2} \text{ s}^{-1}$ . The neckings are quite diffuse and extend widely along the gauge length. Figure 4 also reveals that most samples fracture in a shear mode with an angle of about  $55^\circ$  with respect to the tensile axis except for the one tested at  $10^{-2} \text{ s}^{-1}$ . The latter fractures in a zig-zag fashion with two shear segments making an angle of  $47\text{--}50^\circ$ , which may be caused by the occasional initiation and interconnection of two shear fractures at different locations.

In contrary to the apparent necking at the sample planes, the side-view observations show that the samples exhibit homogeneous deformation in the thickness direction, without any noticeable necking even at the fracture edges (Figure 3e–h). The plastic strain  $\epsilon_t$  in the thickness direction, defined as  $\ln(t_0/t)$ , where  $t_0$  and  $t$  are the original and final sample thickness respectively, increases from only 4.9 to 12% with increasing strain rate. The true strain at the fracture, calculated based on the area reduction near the fracture, substantially increases from  $\approx 20$  to over 70% with increasing strain rate, demonstrating again the capability of plastic straining in the course of high-rate deformation. In comparing the plastic strains in width direction and thickness direction in Figure 4, all the columnar-grained nt-Cu samples exhibit substantial plastic strain anisotropy at all strain rates. This is mainly correlated with the presence of highly aligned nanoscale twins and will be discussed below.

Both the tensile stress–strain curves (Figure 2) and the geometrical measurement (Figure 4) of the fractured samples apparently illustrate the fact that the columnar-grained nt-Cu becomes less ductile at lower strain rates, especially when considering the elongation subsequent to the necking initiation. Generally, the elongation-to-failure is dependent on the strain hardening that suppresses the initiation of localized necking and the subsequent cracking. The latter plays a more important role in limiting the post-necking deformation due to the build-up of tri-axial tensile stress in the necking area, and therefore may be the origin of the significantly reduced ductility in the low strain rate testing.

In order to probe the fracture behavior of the columnar-grained nt-Cu, close SEM inspections were made on the plane and fracture surface of samples tested at different strain rates. Figure 5a displays the sample surface in the vicinity of the fracture of the nt-Cu tested at  $10^{-5} \text{ s}^{-1}$ . Plenty of thin cracks with length smaller than  $10 \mu\text{m}$  and a few large cracks with length exceeding  $50 \mu\text{m}$  are clearly observed. Most cracks make an angle of  $50\text{--}55^\circ$  with respect to tensile direction, and are almost parallel to the final shear fracture direction. The sample surface is still flat without any visible deformation features, which may be associated with the relatively small sustainable strain ( $\epsilon = \approx 20\%$ ). In contrary, the sample surface tested at  $10^{-2} \text{ s}^{-1}$  exhibits evident localized deformation bands and becomes quite rough (Figure 5b). The deformation

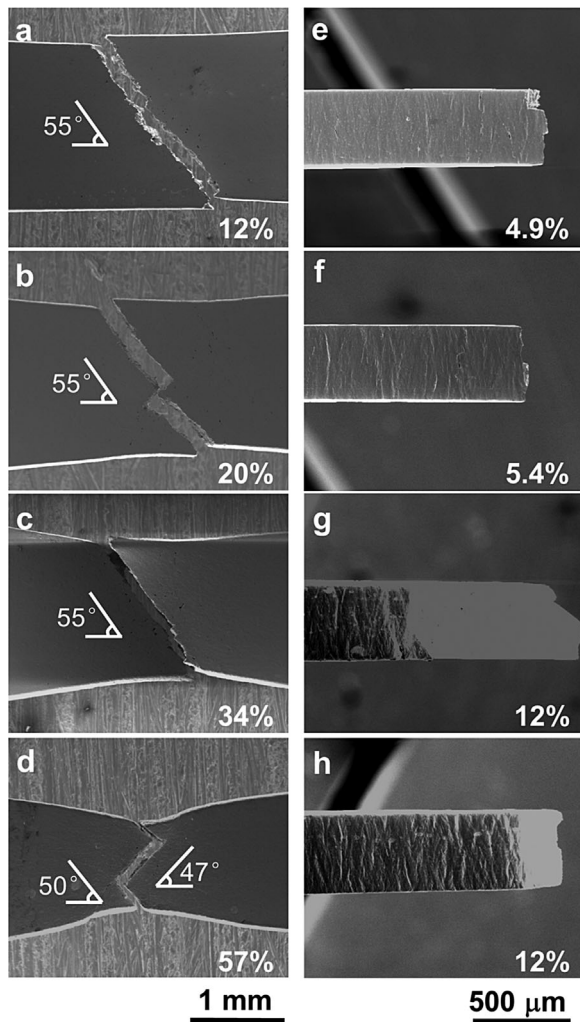


Fig. 4. Geometric dimensions of fractured columnar-grained nt-Cu tested at different strain rates: (a, e)  $10^{-5} \text{ s}^{-1}$ ; (b, f)  $10^{-4} \text{ s}^{-1}$ ; (c, g)  $10^{-3} \text{ s}^{-1}$ ; (d, h)  $10^{-2} \text{ s}^{-1}$ . (a–d) are plane-view observations with a percentage indicating the true strain in width direction, and (e–h) are side-view observations with a percentage indicating the true strain in thickness direction.

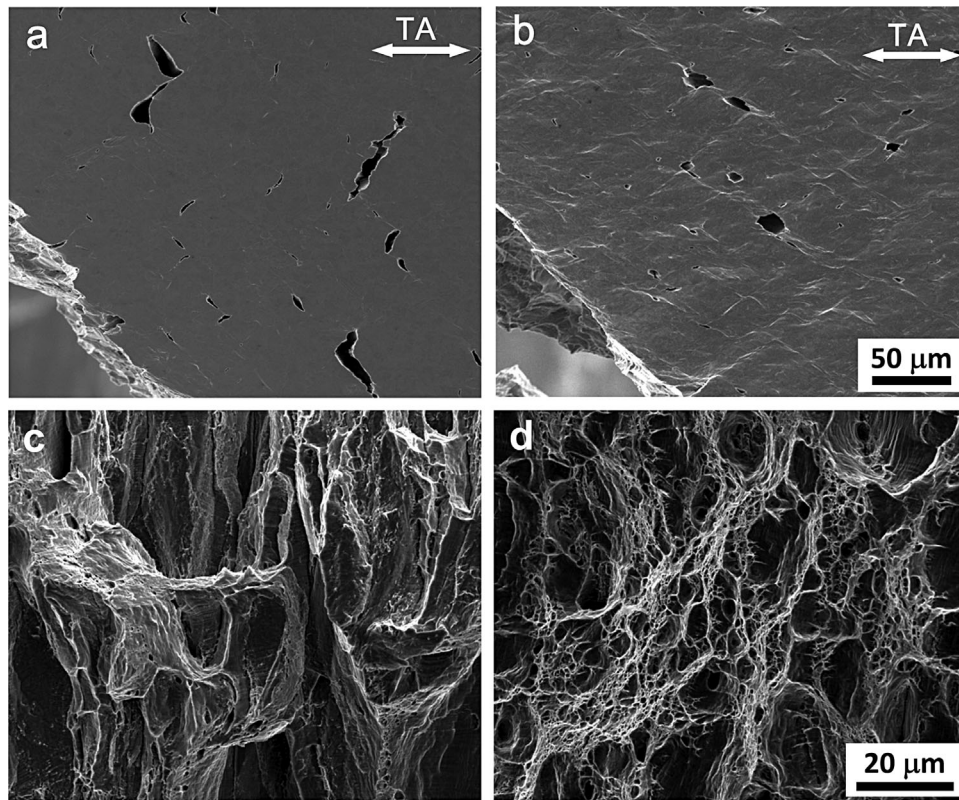


Fig. 5. Sample planes and fracture surfaces of columnar-grained nt-Cu tested at different strain rates: (a, c)  $10^{-5} \text{ s}^{-1}$ ; (b, d)  $10^{-2} \text{ s}^{-1}$ . The double-head arrows TA represent the tensile direction.

bands form two intersecting groups, both making an angle of  $\approx 55^\circ$  with respect to the tensile axis. Figure 5b also shows numerous cracks near the fracture. These cracks are much shorter and wider in comparison to those formed at low strain rates (Figure 5a), and mostly lie at the intersections of two deformation bands.

Figure 5c displays the fractographic observation of columnar-grained nt-Cu tested at  $10^{-5} \text{ s}^{-1}$ . Numerous ridges and corners parallel to the longitudinal direction of the original columnar grains appear to indicate that the samples fracture in an intergranular fashion at low strain rates. As a rough estimate, the fraction of the intergranular fracture area is  $\approx 85\%$ . In contrary, the typical morphology at  $10^{-2} \text{ s}^{-1}$  is conventional ductile fracture dimples, as shown in Figure 5d. There are also a few intergranular fracture surfaces, but the area fraction is below 5%, much smaller than the case of low strain rate testing. Obviously, the fracture process of columnar-grained nt-Cu is strongly dependent on the imposed strain rate. The transition of fracture mode from ductile dimple fracture to brittle intergranular fracture of nt-Cu would occur with decreasing strain rate, which have not been reported previously. The unique strain rate effect of the nt-Cu with highly oriented nanoscale twins may be associated with the preferential TB orientation and the grain size in micrometer scale, which leads to different dislocation behavior that influences the competition between continuous plastic deformation and crack nucleation.

The nanotwinned structure possesses a typical two-dimensional characteristic length scales: the relative large twin length (or grain size), varying from the nanometer to micrometer scale, and the small twin thickness in the nanometer scale.<sup>[9,16]</sup> This microstructural hierarchy leads to a highly anisotropic plastic deformation mechanism associated with dislocation–TB interactions and with the presence of three different dislocation modes, namely dislocation transfer across TBs (mode I), threading dislocation glide in between the TBs (mode II), and partial dislocation-mediated TB migration (mode III).<sup>[9,12]</sup> Note that the dominate dislocation mechanism can be effectively switched among the above three modes by only changing the loading direction with respect to the TB planes.<sup>[12]</sup>

As the case in this study, since the nanoscale TBs are preferentially oriented parallel to the tensile direction, the mode I and mode III mechanisms are constrained due to the small resolved shear stress in these slip systems, and the plastic deformation is therefore governed by threading dislocations in mode II.<sup>[11,12]</sup> For this deformation mode, computer simulations reveal that dislocations usually nucleate near GBs, bow out and transverse through the slender twin lamellae, and then stop near GBs at the opposite side of the twin lamella.<sup>[9,12]</sup> Therefore, dislocation activities in the vicinity of GBs accommodate the major plastic strain of the highly aligned nt-Cu, especially when the imposed strain is large, as demonstrated by the experimental observations on

the columnar-grained nt-Cu sample deformed at a high strain rate of  $5 \times 10^{-3} \text{ s}^{-1}$ .<sup>[11]</sup> It was revealed that the deformation tends to become inhomogeneous with increasing tensile strain. The strain inhomogeneity, along with intensive accumulation and rearrangement of dislocations (forming cells or subgrains) and with detwinning behavior as well, results in a much larger strain at GBs than that sustained by grain interiors.<sup>[11]</sup>

The present observations of pronounced strain rate effect on the fracture mode of columnar-grained nt-Cu may also be associated with the evolution of dislocation structures in the vicinity of GBs. In general, stress concentration at GBs in metals can be plastically relaxed by easy activation of multiple slip systems in adjacent grains. But, as discussed above, the highly aligning of nanoscale TBs with the tensile direction will result in restriction on certain slip systems, especially dislocation in the mode III that glide under lower resistance at TBs.<sup>[27,28]</sup> Fortunately, the concentrated plastic strain near GBs is prone to accumulate high-density dislocations and create substructures at the high strain rate case. The formation of dislocation substructures in the vicinity of GBs can further realize a larger degree of stress relaxation. As a consequence, the nt-Cu sample fractures through void nucleation and coalescence at high strain rates, generating numerous fine ductile dimples (see Figure 5d).

However, this is not the case at low strain rates, which shows obvious intergranular cracking in a less ductile manner (Figure 5c). The most probable explanations are related to the dislocation annihilation and the detwinning near GB regions, which should precede the formation of dislocation substructures or subgrains, and both processes are greatly sensitive to the imposed strain rate. Therefore, reducing strain rate will restrict the detwinning process and deter the formation of GB substructures, and thus increasing propensity of nucleation and relatively fast propagation of intergranular cracks are expected. Detailed characterizations on the microstructural evolution at GB region of the columnar-grained nt-Cu are in progress.

At low strain rates, based on the speculation of insufficient plastic relaxation, the nucleation and propagation of intergranular cracks will be controlled by the magnitude of GB stress concentration, which essentially stems from the pileup of threading dislocations on the slip planes. This implies that the GB cracking is strongly dependent on the grain size, as analyzed below. The number of dislocations in a pileup is  $n \propto \tau d$ , where  $\tau$  is the applied shear stress and  $d$  is the grain size, representing the length of the pileup.<sup>[29]</sup> For the threading dislocations in the nanotwinned lamellae,  $\tau \propto 1/\lambda$ , where  $\lambda$  is the twin thickness.<sup>[11]</sup> Then the stress acting at the head of the piled-up dislocations is  $n\tau \propto d/\lambda^2$ . In the nt-Cu prepared by magnetron sputtering,  $d \approx 500 \text{ nm}$ ,  $\lambda \approx 50 \text{ nm}$ , and  $d/\lambda^2 \approx 0.2 \text{ nm}^{-1}$ ,<sup>[22]</sup> but for the samples in this study,  $d \approx 6000 \text{ nm}$ ,  $\lambda \approx 70 \text{ nm}$ , and  $d/\lambda^2 \approx 1.2 \text{ nm}^{-1}$ . Therefore, the dislocation pileups against GBs in present samples with relatively large grains will cause a stress concentration six times that in samples with submicron grains.<sup>[22]</sup> This explains the reason

why the significant strain rate effect on the ductility and fracture behavior was not observed in previous studies, since the much smaller stress concentration could be completely relaxed by deformation at GB areas. In contrary, the incapability to fully release the GB stress concentration would inevitably elevates the susceptibility to intergranular fracture in nt-Cu with coarse grains of micrometer size.

In summary, the present work examines the effect of strain rate on the tensile ductility and fracture behavior of a bulk columnar-grained nt-Cu with highly aligned nanoscale twins. The tensile ductility, especially the post-necking ductility, is strongly dependent on the imposed strain rate. The substantial decrease in the overall elongation at low strain rates is closely correlated with the evident intergranular cracking.

### 1. Experimental Section

The high-purity (99.998 at%) columnar-grained nt-Cu samples with highly oriented nanotwins were prepared by a direct-current electrodeposition technique in an electrolyte of  $\text{CuSO}_4$ . The detailed preparation procedure and parameters have been described elsewhere.<sup>[11]</sup> The total deposition time was about 24 h to obtain samples with average thickness of  $\approx 500 \mu\text{m}$ . X-ray diffraction analysis verified the existence of a strong  $\{111\}$  out-of-plane texture. Dog bone-shaped flat tensile samples with a gauge length of 5 mm and a gauge width of 2 mm were cut from the as-deposited Cu sheets using an electric spark machine and then mechanically polished to a final thickness of  $\approx 400 \mu\text{m}$  from the growth surface. All the samples were further chemically polished to minimize the surface roughness and to remove the thin hardening layer caused by mechanical polishing. Uniaxial tensile tests were performed on an Instron 5848 microtester at RT ( $\approx 300 \text{ K}$ ) with four different strain rates,  $10^{-5}$ ,  $10^{-4}$ ,  $10^{-3}$ , and  $10^{-2} \text{ s}^{-1}$ . A contactless MTS LX300 laser extensometer was used to accurately measure the strain of the sample upon loading. After tensile testing, morphologies of the sample plane and fracture surfaces were examined in a field emission gun SEM (FEG-SEM, FEI Nova NanoSEM 430) with secondary electron imaging mode.

Received: February 9, 2015

Final Version: March 15, 2015

- [1] K. Lu, L. Lu, S. Suresh, *Science* **2009**, 324, 349.
- [2] L. Lu, X. Chen, X. Huang, K. Lu, *Science* **2009**, 323, 607.
- [3] K. Lu, F. K. Yan, H. T. Wang, N. R. Tao, *Scr. Mater.* **2012**, 66, 878.
- [4] Y. Wei, Y. Li, L. Zhu, Y. Liu, X. Lei, G. Wang, Y. Wu, Z. Mi, J. Liu, H. Wang, H. Gao, *Nat. Commun.* **2014**, 5, 3580.
- [5] I. J. Beyerlein, X. Zhang, A. Misra, *Annu. Rev. Mater. Res.* **2014**, 44, 329.
- [6] Z. H. Jin, P. Gumbsch, K. Albe, E. Ma, K. Lu, H. Gleiter, H. Hahn, *Acta Mater.* **2008**, 56, 1126.

- [7] L. Lu, Z. S. You, K. Lu, *Scr. Mater.* **2012**, *66*, 837.
- [8] X. Li, Y. Wei, L. Lu, K. Lu, H. Gao, *Nature* **2010**, *464*, 877.
- [9] T. Zhu, H. Gao, *Scr. Mater.* **2012**, *66*, 843.
- [10] L. Zhu, H. Ruan, X. Li, M. Dao, H. Gao, J. Lu, *Acta Mater.* **2011**, *59*, 5544.
- [11] Z. S. You, L. Lu, K. Lu, *Acta Mater.* **2011**, *59*, 6927.
- [12] Z. You, X. Li, L. Gui, Q. Lu, T. Zhu, H. Gao, L. Lu, *Acta Mater.* **2013**, *61*, 217.
- [13] Q. S. Pan, Q. H. Lu, L. Lu, *Acta Mater.* **2013**, *61*, 1383.
- [14] L. Lu, Z. S. You, *Acta Metall. Sin.* **2014**, *50*, 129.
- [15] R. J. Asaro, S. Suresh, *Acta Mater.* **2005**, *53*, 3369.
- [16] M. Dao, L. Lu, Y. F. Shen, S. Suresh, *Acta Mater.* **2006**, *54*, 5421.
- [17] T. Zhu, J. Li, A. Samanta, H. G. Kim, S. Suresh, *Proc. Natl. Acad. Sci. USA* **2007**, *104*, 3031.
- [18] L. Lu, R. Schwaiger, Z. W. Shan, M. Dao, K. Lu, S. Suresh, *Acta Mater.* **2005**, *53*, 2169.
- [19] L. Lu, M. Dao, T. Zhu, J. Li, *Scr. Mater.* **2009**, *60*, 1062.
- [20] L. Lu, T. Zhu, Y. Shen, M. Dao, K. Lu, S. Suresh, *Acta Mater.* **2009**, *57*, 5165.
- [21] J. C. Ye, Y. M. Wang, J. T. W. Barbee, A. V. Hamza, *Appl. Phys. Lett.* **2012**, *100*, 261912.
- [22] A. M. Hodge, Y. M. Wang, T. W. Barbee Jr., *Scr. Mater.* **2008**, *59*, 163.
- [23] X. H. Chen, L. Lu, K. Lu, *Scr. Mater.* **2011**, *64*, 311.
- [24] X. Zhang, A. Misra, H. Wang, T. D. Shen, M. Nastasi, T. E. Mitchell, J. P. Hirth, R. G. Hoagland, J. D. Embury, *Acta Mater.* **2004**, *52*, 995.
- [25] L. Lu, Y. Shen, X. Chen, L. Qian, K. Lu, *Science* **2004**, *304*, 422.
- [26] Y. F. Shen, L. Lu, Q. H. Lu, Z. H. Jin, K. Lu, *Scr. Mater.* **2005**, *52*, 989.
- [27] H. Zhou, S. Qu, *Nanotechnology* **2010**, *21*, 035706.
- [28] I. Shabib, R. E. Miller, *Acta Mater.* **2009**, *57*, 4364.
- [29] M. A. Meyers, K. K. Chawla, in *Mechanical Behavior of Materials*, Ed. V 2, Cambridge University Press, Cambridge, UK **2009**, Ch. 5.